



A study on the effect of directed energy deposition substrate energy on clad geometry

Jessica Dill¹ · Masakazu Soshi¹ · Kazuo Yamazaki¹

Received: 23 December 2019 / Accepted: 14 May 2020 / Published online: 1 July 2020
© Springer-Verlag London Ltd., part of Springer Nature 2020

Abstract

Directed energy deposition (DED) is an additive manufacturing (AM) process where a laser is used to fuse a metal powder onto a substrate. The powder is deposited in a layer-by-layer fashion, and each deposited track is referred to as the clad. Large thermal gradients that occur during DED can cause changes in the clad geometry as well as deformation of the substrate and final part. Thermal behavior of DED manufactured parts and mitigation of thermal distortion has been addressed in the literature, but these studies mainly focused on material properties while neglecting the effect of thermal distortion on part geometry. One of the mitigation strategies that has been widely tested and accepted is substrate preheating. This study uses analytical and experimental models to observe changes in clad geometry when energy input to the part is varied by adjusting process parameters and preheating the substrate. A method to quantify substrate energy, or the amount of heat energy the substrate holds, is found as well as a relationship between the substrate energy and clad geometry. The geometry of the clad can be controlled by controlling the total energy added to the clad.

Keywords Additive manufacturing · Direct energy deposition · Clad geometry · Substrate preheat

1 Introduction

Additive manufacturing (AM) is a group of modern manufacturing methods that can produce three dimensional products from computer-aided design (CAD) models. These technologies generally involve the addition and bonding of materials in a layered manner to form parts. The 3D geometric data from the CAD model is divided into layer data, and the layers are constructed using a machine with AM capabilities [1].

1.1 Introduction to directed energy deposition

There are many different forms of AM. Some processes direct thermal energy from laser beams using optics to melt or sinter metal or plastic powder together. Others use inkjet-type printing heads to spray a binder or solvent onto the powdered

material [1]. One of these major AM processes is direct energy deposition (DED).

DED is any type of metal additive manufacturing where a heat source is used to melt a material feed and fuse it onto a surface as it is deposited. The type of DED used in this research involves a high-powered laser beam that melts a stream of powdered metal onto a substrate as shown in Fig. 1. The laser and powder stream move together to form a specified part geometry. The substrate is fixed on a table that can rotate along two axes so that it can be positioned properly for unique geometries. As the material is deposited onto the substrate, a melt pool forms on the surface, which includes a portion of the powdered metal and substrate material that are in the liquid state. This bonds the powder to the substrate as the material cools and solidifies. This deposition process is repeated layer by layer to build the desired part. DED does not produce as high-quality surface finishes as other types of AM and typically requires post-process machining to ensure correct part dimensions. Otherwise, DED is a relatively fast process that allows for the fabrication of complex part geometries.

The DED process is dependent on several operating parameters. Some of the significant process parameters are laser transverse speed, laser power, powder feed rate, interlayer dwell time (the amount of time that the laser is turned off

✉ Masakazu Soshi
msoshi@ucdavis.edu

¹ University of California Davis, 1 Shields Ave,
Davis, CA 95616, USA

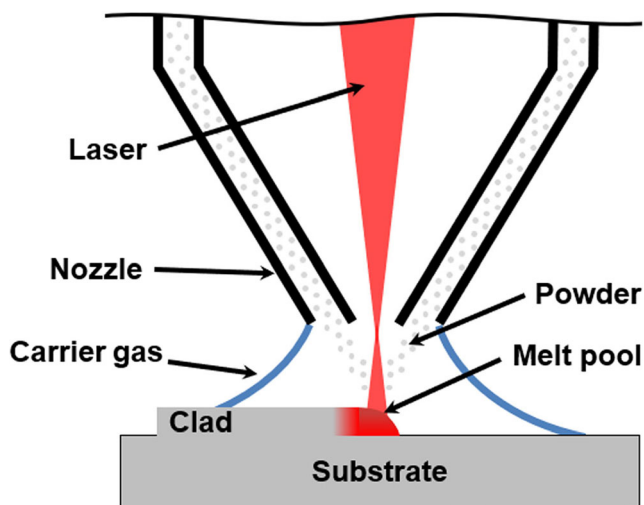


Fig. 1 Direct energy deposition process

between layers), and step over distance (the amount of overlap between two adjacent deposited tracks). The values of these parameters may need to be adjusted based on the materials being used or the type of part being built [2].

Powder-based DED machines can either have one or multiple nozzles as part of a powder delivery system to introduce the continuous powder stream along with the laser beam. The powdered metal is stored in a pressurized container, and it is mixed with a carrier gas in order to be transported through the powder feed line. The material coming from the powder nozzle intersects with the laser beam at the laser focal point. The focus of the laser can be adjusted to change the size of the laser spot. Different DED machines can have different types of lasers with various power ranges. The energy delivery per unit area of material for a specific process can be measured by calculating the energy flux (kJ/cm^2) or EF. This parameter is useful because it can be used to predict layer geometry. The energy flux equation is shown in Eq. 1 where P is the laser power (W), v is the traverse speed (mm/min), and d is the laser beam diameter (mm) [2].

$$EF = \frac{P}{dv} \quad (1)$$

Some DED machines use solid state or diode lasers with powers usually on the order of a few kilowatts and laser spot diameters on the order of millimeters. Laser power attenuation occurs during deposition because the powder absorbs and scatters some of the radiation. The amount of attenuation can be significant, and the highest attenuation occurs near the center of the laser beam. The absorptivities of the powdered material and the substrate surface affect how much of the laser radiation is absorbed into the melt pool. It is difficult to predict or measure the absorptivity values and how they change during deposition. Therefore, many DED simulations model the laser attenuation and melt pool absorption using a

total absorption coefficient to scale the laser power input so that the actual power that is delivered to the melt pool can be approximated. This coefficient can range between 0.15 and 0.5 and depends on a multitude of factors [2].

The melt pool is an approximately spherical droplet that moves at the traverse speed of the laser. It changes in size and internal energy during deposition due to surrounding heat transfer and the variability of the process. The melt pool is what eventually creates the solid part, which means that its temperature and shape are very important in terms of accuracy and consistency of the final part. Part geometry depends on the melt pool behavior during the build process. Geometry of the clad, which is one track of deposited material after it has cooled and solidified, also depends on melt pool behavior. Due to the continuous powder addition, the temperature and movement of the melt pool are not always consistent, making it difficult to control final part geometry [2].

1.2 Literature review

Distortion in additively manufactured parts due to spatially variable heating and cooling is a well-known problem that has already been addressed in the literature [3–14]. Many analytical models have been created to model thermal behavior in the different methods of additive manufacturing [3–8]. Foteinopoulos et al. [3] developed a two-dimensional finite difference model for the thermal history of powder bed fusion manufactured parts. They used temperature-dependent material properties and monitored the temperature over time for different nodes across a multilayer part. Their results can be used to adjust the process parameters, such as laser power, traverse speed, and laser offset, in order to increase efficiency [3]. A three-dimensional finite element model was created by Majeed et al. [4] to model the melt pool characteristics during selective laser melting (SLM). Temperature-dependent material properties were also used, and the effects of process parameters on thermal variables were analyzed. The results from Majeed et al. showed that a high energy density, i.e., high laser power and low scan speed, resulted in higher maximum melt pool temperatures. They also found that the thermal gradient is at a maximum between the substrate and first layer and increases along each layer [4]. Other similar finite element models for SLM have been developed as well. Huang and Zhang [5] and Huang et al. [6] both created finite element models of thermal behavior in SLM. Huang and Zhang monitored the thermal behavior in thin wall parts using ANSYS. Temperature-dependent material properties were used. They found that the width and depth of the melt pool increase in the higher layers of a part. This is due to heat accumulation as more layers are added to a part [5]. The model that Huang et al. created was similar, but they analyzed how the laser power and scan speed affect the dimensions of the melt pool. They found that all melt pool dimensions increase when laser

power increases or scan speed decreases. It was concluded that increasing laser power is more effective than reducing scan speed when trying to change the melt pool temperature or size [6].

Manvatkar et al. [7] created a heat transfer and fluid flow model of the DED process in multilayer parts. They also used temperature-dependent material properties and looked at the size and temperature of the melt pool. In agreement with other simulations, the melt pool size continues to increase in the upper layers of a part. The maximum temperature of the melt pool also increases as number of layers increases. They found that the cooling rate continuously and significantly decreases in the upper layers. They believe that this is due to the reduced rate of heat transfer to the substrate because the substrate acts as a heat sink in the initial layers [7].

The thermal behavior has a relationship with the process parameters used in DED and the final part quality. Yan et al. [8] studied the effects of laser power, scan speed, and powder flow rate on the thermal behavior and resulting product quality. Higher laser power and slower scanning speed both correspond with an increase in temperature of the melt pool. The length, width, and depth of the melt pool also consistently increased with increased laser power and decreased scan speed. Rapid temperature cycling during the deposition process causes a high temperature gradient around the melt pool, which results in unwanted dimensional distortion in the substrate and the part. This deformation is typically monitored after processing using laser metrology scanning. It was found that layer thickness and heat input influence the deformation and that the maximum temperature gradient occurs between layers due to the large cooling rate of the previous track [8].

Many methods to alleviate thermal distortion have been proposed, but none have been widely established. One method proposed by Tang and Landers [9] focused on the fact that fixed process parameters are used during laser metal deposition. With constant parameters such as laser power, due to the increase in substrate temperature as deposition goes on, tracks become nonuniform and thermal distortion increases. Tang and Landers note that regulating heat input is important. Their method was to control the melt pool temperature for each layer by adjusting the laser power profile between layers. Average melt pool temperature and height data were recorded for the previous layer, and the laser power profile was calculated from this data using iterative learning control. Their experiments showed that layer-to-layer temperature control produces a more uniform clad morphology than constant laser power deposition [9].

Preheating of the base material, either localized or globalized, has been shown to mitigate some of the negative side effects of the high cooling rate during DED [10–12], but the full relationship between preheating and clad geometry is not

yet known. Substrate preheating of up to 1000 °C was used by Muller et al. [10] for powder bed-based laser beam melting of pure tungsten powder onto pure tungsten substrate plates. They used an induction heating system and tested temperatures of 600, 800, and 1000 °C. They mainly analyzed the mass density and microstructure of the samples. Their results showed that elevated substrate temperatures are beneficial for material consolidation. The maximum preheat temperature samples showed a lower crack density than non-preheated samples, although some macroscopic defects are still visible in the preheated sample. They did not look at the effect of preheating on the geometry of the parts [10].

Zhang et al. [11] also used the substrate preheating method to build thin-wall parts and evaluated the surface quality, microstructure, and mechanical properties of the parts. They deposited Ni60A alloy powder onto Q235 steel substrates with different thicknesses. The preheating temperatures ranged from 300 to 600 °C. All DED parameters other than preheat temperature remained constant for all experiments. They found that for higher preheat temperatures, the width of the wall increased. This was due to a higher deposition rate at higher preheat temperatures, which means that more powder is being melted. They also found that positive deflection of the substrate became more significant at higher temperatures because of the thermal stresses being transferred to tensile stress in the cooling phase. The surface finish of the parts showed that cracks formed on the surface at lower temperatures and higher preheat temperatures resulted in a finer surface finish and better forming quality [11].

Fallah et al. [12] performed a similar analysis but with localized preheating of the substrate before deposition. The idea was that for certain applications, preheating the entire substrate may not be possible. They used Stellite 1 powder and AISI-SAE 4340 alloy steel substrates. For preheating, the laser spot diameter was set to 7.6 mm, and the laser beam scanned the surface of the substrate in a predefined path immediately before deposition. The laser was able to heat the surface to about 400 K. Their results showed a crack-free surface for the preheated substrate compared to macroscopic cracks on the non-preheated surface. The maximum melt pool temperature was higher for the preheated sample, which indicates a larger melting boundary and higher powder catchment. But due to preheating, a more uniform temperature distribution and smaller temperature gradients were obtained in spite of the higher maximum temperatures. The preheated sample cross section appeared much thicker and more uniform than the non-preheated sample [12]. All of these substrate preheating studies showed the benefits of preheating on the development of the melt pool, temperature gradients, and cooling rates, but none analyzed the final geometry of the parts in depth or the relationship between preheating and clad geometry.

1.3 Scope of research

1.3.1 Motivation

Additive manufacturing can increase productivity while reducing material usage and cost and provide the ability to manufacture complex part geometries. The advantages of AM have caused the interest and applications of AM technology to increase in recent years. The aerospace, automotive, energy, and medical industries are beginning to use AM to fabricate fully functional metal components. With increased demand for AM parts, it is very important to make the process as efficient and accurate as possible.

One major disadvantage of DED is that very large thermal gradients occur during deposition which cause deformation in both the substrate and the deposited part. Rapid heating and cooling of the material makes it difficult to maintain consistent and accurate clad geometry for each deposited layer. It is desirable for AM parts to be overbuilt so that post-process machining can be used to achieve required geometric tolerances. However, parts can often be underbuilt, which requires another round of DED to deposit the missing material. If original parts manufactured using DED can be built more consistently and accurately, this will reduce the amount of post-process machining or rebuilding necessary to maintain accurate part geometry and make the overall process more efficient [15].

The melt pool is a part of both the substrate and the clad area. Therefore, the energy within the melt pool is a factor of the laser energy and the substrate energy. The energy within the substrate is influenced by the substrate temperature. A formula representing this relationship is shown in Eq. 2:

$$Q_{melt\ pool} = Q_{wp} - Q_{substrate} - Q_{other} \quad (2)$$

where $Q_{melt\ pool}$ is the laser energy absorbed by the melt pool (kJ), Q_{wp} is the laser energy absorbed by the workpiece, $Q_{substrate}$ is the energy absorbed by the substrate, and Q_{other} includes any other loss of energy through conduction, radiation, etc. Looking at substrate energy in terms of conduction gives:

$$\frac{\partial Q_{substrate}}{\partial t} = k \cdot A \cdot grad(T) \quad (3)$$

where k is the conduction coefficient of the substrate (W/m·K), A is the conduction area (cm²), $grad(T)$ is the temperature gradient (K), and t is time (s). The temperature gradient between the substrate and the melt pool decreases if the temperature of the substrate increases, so according to Eq. 3, the amount of energy absorbed by the substrate decreases as substrate temperature rises. Rewriting Eqs. 2 and 3 gives:

$$Q_{melt\ pool} = Q_{wp} - \int k \cdot A \cdot grad(T) - Q_{other} \quad (4)$$

Assuming that the laser energy remains constant for most DED processes, the melt pool energy should increase as substrate temperature increases.

1.3.2 Objective of research

Due to changes in clad geometry in the upper layers of multilayer parts built using DED, the current hypothesis is that if the total energy being added to the clad from both the laser and the substrate can be kept constant, then the clad geometry can be kept constant. The objective of this project is to find the relationship between clad geometry and total clad energy to see if this theory is correct. The total clad energy (kJ) is defined by the following equation:

$$Q_T = Q_{laser} + Q_{substrate} \quad (5)$$

The laser energy is a known quantity that can be calculated using DED input parameters. Laser energy is given by:

$$Q_{laser} = EF \cdot A \quad (6)$$

where EF is the energy flux, calculated using Eq. 1, and A is the area of the laser spot (cm²). The substrate energy, or the amount of heat energy the substrate contributes to the clad, is an unknown value and is variable for each layer. If a method to quantify the substrate energy can be determined, the total clad energy can be measured and controlled in a way that allows for consistent and accurate clad geometry.

1.4 Approach

1.4.1 Overview

The relationship between the clad energy and clad geometry is analyzed using simulations as well as experiments. The simulations will be used to observe trends in the data and gain insight on how the results might change prior to performing experiments. Two different types of simulations will be completed: substrate preheat simulations and laser power modulation simulations. Substrate preheat and laser power modulation experiments will also be performed.

1.4.2 Substrate preheat tests

In the substrate preheat tests, the substrate is heated prior to deposition to a predefined temperature. The substrate remains the same size, and all of the deposition parameters, including the laser power, are kept constant for each test. The purpose of these tests is to observe how the clad geometry changes when energy is added to it from the substrate as well as from the laser. This process simulates deposition at different layers throughout the stages of fabrication of a part.

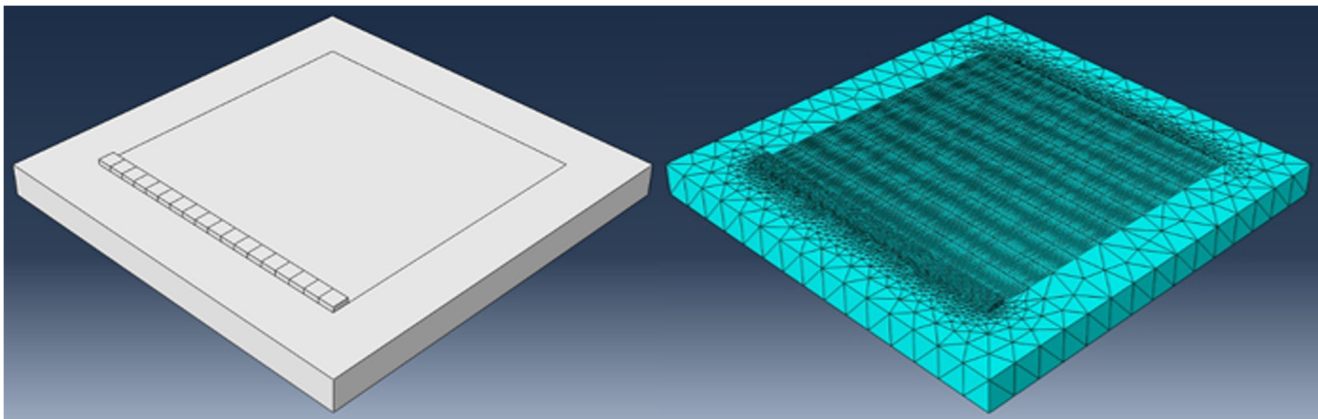


Fig. 2 Simulated substrate and clad placement (left) with mesh (right)

1.4.3 Laser power modulation tests

In the laser power modulation tests, the substrate is still preheated, but the laser power is also adjusted for each test. All other deposition parameters stay the same. As the substrate temperature increases, the laser power is decreased so that the laser energy flux is decreased. The amount to lower the laser power by for each test is estimated using the previous experimental lab data. The purpose of these tests is to keep the melt pool and clad geometry constant for each substrate

Table 1 Material properties for 316-L stainless steel [13, 14, 16]

Temperature (°C)	Thermal conductivity (W/m·K)	Density (g/cm ³)	Expansion coefficient (10 ⁻⁶ /K)	Latent heat (kJ/kg)	Specific heat (J/kg·K)
23	13.5	7.95	15.9	260	470
100	15.5	–	15.9	–	490
200	17.6	–	–	–	520
300	19.4	–	16.3	–	540
400	21.8	–	–	–	560
500	23.4	–	19.3	–	570
600	24.5	–	–	–	590
700	25.1	–	–	–	600
800	27.2	–	–	–	630
900	27.9	–	–	–	640
1000	29.1	–	–	–	660
1100	29.3	–	–	–	670
1200	30.9	–	–	–	700
1300	31.1	–	–	–	710
1385	31	–	–	–	720
1450	28.5	–	–	–	830
1500	29.5	7	–	–	–
1600	30.5	–	–	–	–
2000	–	6.6	–	–	–

temperature to test the theory that maintaining a constant total clad energy will produce constant geometry.

2 Numerical study of substrate preheating

2.1 Simulation overview

Directed energy deposition simulations were created using finite element analysis with the commercial software package Abaqus. The simulations modeled a single track, single layer deposition. The model consisted of a substrate, a clad, a moving surface heat flux to represent the laser, surface film conditions to model heat transfer between the materials and surroundings, and an initial temperature condition on the substrate to represent the preheating.

2.1.1 Mesh and material properties

The substrate was modeled as a solid 74 mm square by 6 mm thick part. The clad was modeled as a solid 54 mm by 3 mm by 1 mm thick section that was positioned on top of the substrate as shown in Fig. 2. The clad was divided into 18 sections, each

Table 2 Initial substrate temperatures used in simulations

Initial substrate temperature (°C)
23
100
200
300
400
500
600
700
750

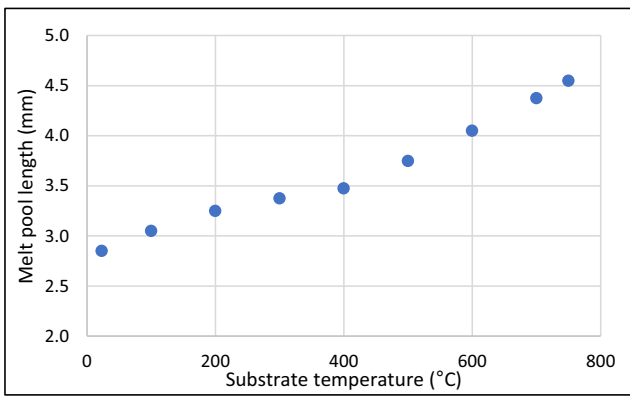


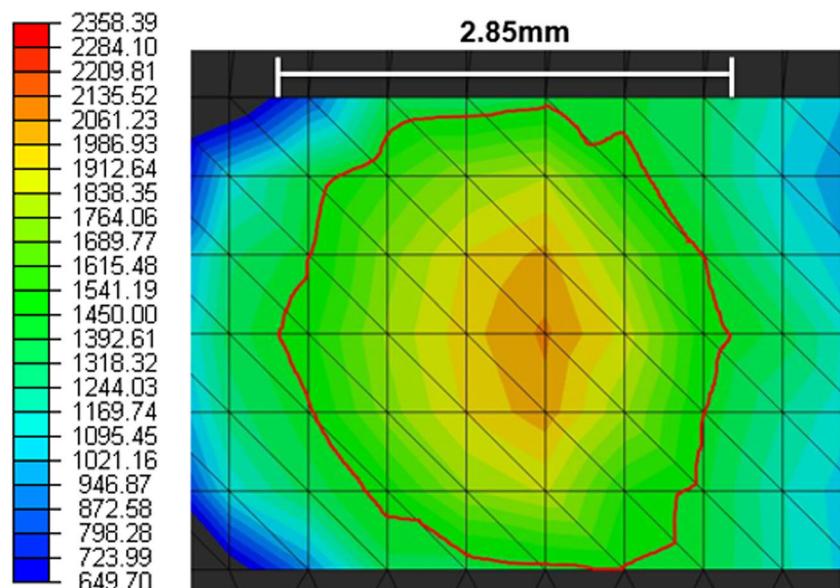
Fig. 3 Melt pool length results versus substrate temperature

3 mm square, and was initially inactive. A linear tetrahedral mesh with 5836 nodes and 24,311 elements was used with an element length of 5 mm on the substrate and an element length of 0.5 mm on the clad section as shown in Fig. 2. The mesh size for the clad section was chosen because a convergence test was performed, and the change in the temperature results at any given node was less than 1% between a 0.5 and 0.25 mm mesh. Results were only obtained for the locally meshed clad section. Three hundred sixteen-liter stainless steel was used for both the substrate and clad materials. Material properties for 316-L stainless steel that were used for both the substrate and clad materials are shown in Table 1. The solidus and liquidus temperatures of 316-L stainless steel are 1385 °C and 1450 °C, respectively [13, 14, 16].

2.1.2 Heat transfer

Heat transfer between the substrate and clad material and their surroundings was modeled using a lumped capacitance model

Fig. 4 Room temperature substrate simulation melt pool with 1200 W



that assumes the substrate has a roughly uniform internal temperature and no internal heat generation [17]. A temperature-dependent coefficient ranging from 0.0121 W/m²K at 0 °C and 0.1921 W/m²K at 3000 °C that combines the heat transfer due to convection and radiation was calculated for the top surface and base/side surfaces based on temperature data collected from the previous DED experiments. Conduction between the substrate and fixture was neglected because the experimental fixture minimizes contact with the work piece.

2.1.3 Laser modeling

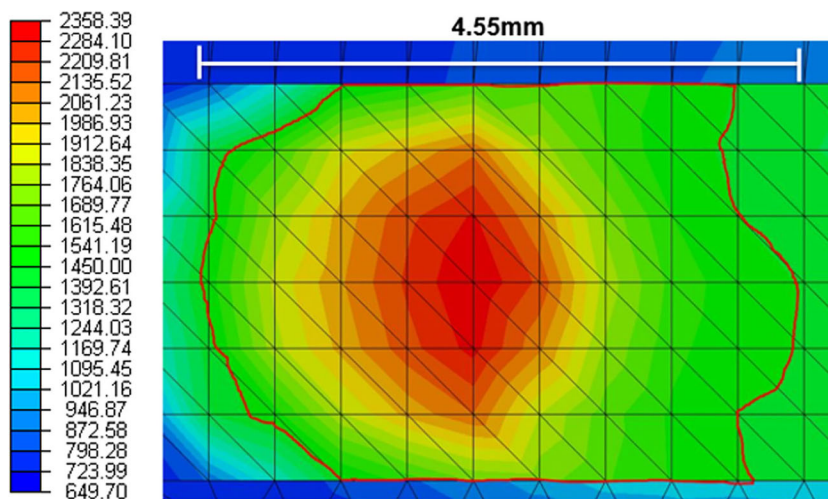
Abaqus allows input of FORTRAN subroutines to model boundary conditions. The laser was modeled as a surface heat flux using a subroutine that controls the laser path. The laser was only applied to the clad section surface in a single line. Each 3 by 3 mm clad section was only activated once the laser passed over it to simulate the deposition of material with the laser. An overall absorption coefficient of 0.42, η , due to laser beam attenuation, absorptivity of the surface, and efficiency of the laser was estimated using information from [2, 18, 19]. Laser power incident on the clad surface was calculated using Eq. 7, where q_0 is the programmed laser power.

$$q = q_0 \eta \quad (7)$$

2.1.4 Initial condition for preheat

An initial temperature condition was placed on the substrate material only to represent the preheating of the substrate. The entire substrate was preheated to a uniform, constant temperature. The initial temperatures that were

Fig. 5 750 °C substrate simulation melt pool with 1200 W



tested are shown in Table 2. The maximum temperature of 750 °C was chosen to avoid any plastic deformation of the substrate after deposition. Plastic deformation is based on stress, but in the case of deformation due to a thermal gradient it is based on whether the yield stress of stainless steel is exceeded. If the substrate temperature is increased above 750 °C the yield stress decreases considerably, and it would be more susceptible to yielding because of the thermal gradients present during the DED process [13].

2.2 Substrate preheat simulations

The first round of simulations involved preheating the substrate to each set temperature from Table 2 and maintaining a constant laser power of 1200 W and feed rate of 1000 mm/min. These simulations were used to observe the effects of substrate temperature on melt pool geometry and to determine a method to quantify the substrate energy, which will be defined in a later section. Results for the melt pool length are shown in Fig. 3. Length of the melt pool is used as an overall melt pool size indicator because width of

the melt pool is restricted to 3 mm due to the width of the clad section of the model.

The results showed an increasing linear trend in the total melt pool size as substrate temperature rises. This makes sense because more energy is being added to the clad from the substrate at higher substrate temperatures. Figures 4 and 5 show the room temperature and maximum temperature substrate simulation results, respectively. The melt pool is outlined in red. These figures show how the temperature distribution and length of the melt pool changes with substrate temperature.

2.3 Laser power modulation simulations

The second round of simulations also included the substrate preheat, but the laser power was decreased as the substrate temperature was increased. The feed rate was kept constant at 1000 mm/min, but the laser power was decreased from 1200 W at room temperature as necessary to achieve the desired melt pool geometry. The parameters used for these simulations are shown in Table 3. These simulations were used to

Table 3 Parameters used in laser power modulation simulations

Initial substrate temperature (°C)	Laser power (W)
23	1200
100	1180
200	1140
300	1100
400	1050
500	1000
600	940
700	870
750	830

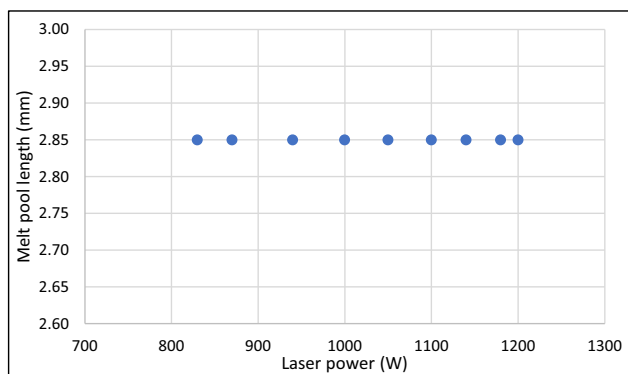
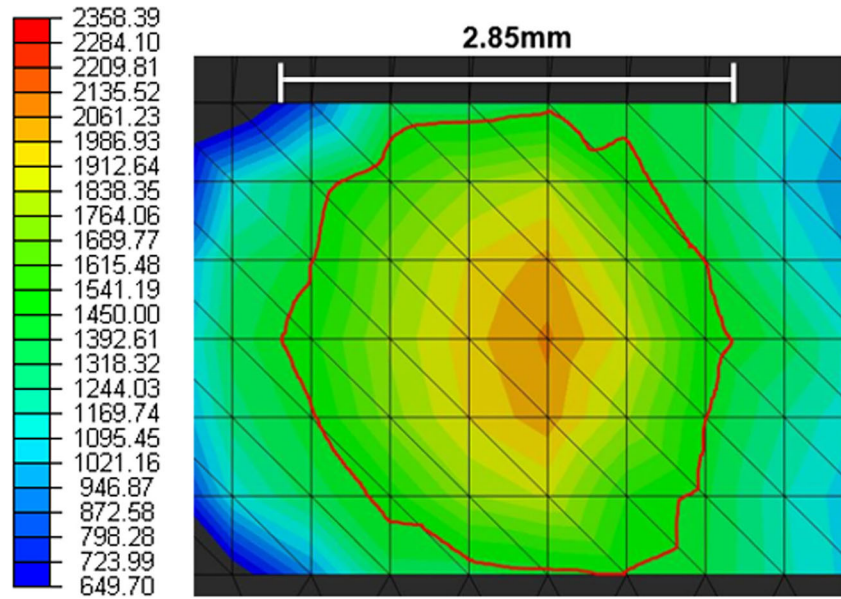


Fig. 6 Melt pool length versus laser power with substrate preheating

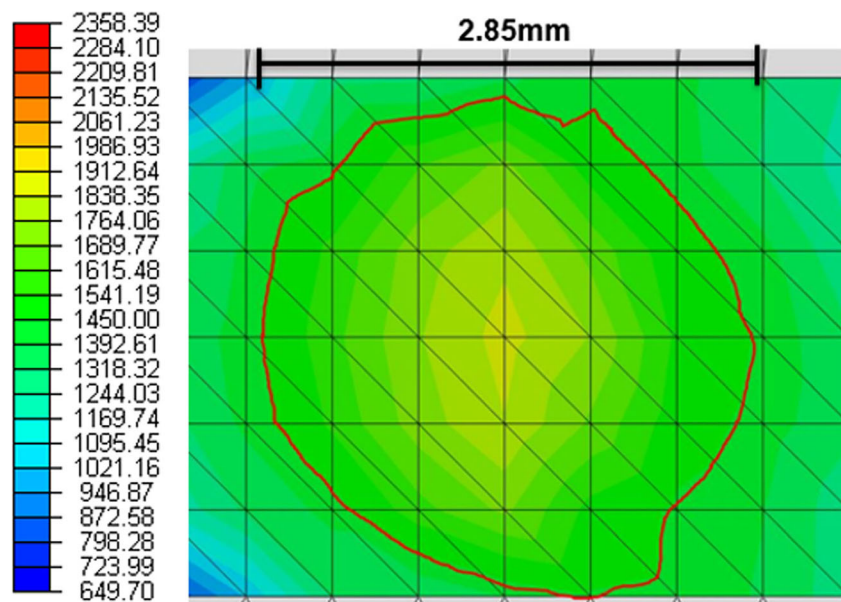
Fig. 7 Room temperature substrate simulation melt pool with 1200 W



test the idea that maintaining constant total energy (as described in Section 1.3.2.) would keep melt pool geometry constant. The results are shown in Fig. 6.

The results of these simulations show that the total melt pool size was able to be kept constant for all values of laser power. The lowest and highest substrate temperature melt pool results, with the melt pool outlined in red, are shown in Figs. 7 and 8 to illustrate that the melt pool size is consistent between the two substrate temperatures. This data shows that it is possible to control the melt pool size by adjusting substrate temperature and laser power.

Fig. 8 750 °C substrate simulation melt pool with 830 W



3 Experimental process and materials

3.1 Experiments overview

Directed energy deposition experiments were performed using the LASERTEC 65 3D Hybrid machine tool, manufactured by DMG Mori. Hybrid means that it has both additive and subtractive machining capabilities. It features a 2500 W fiber coupled diode laser and two powder hoppers that feed powder to a coaxial nozzle with a diameter of 3.1 mm [20].

Table 4 Chemical composition of argon gas in ppm by volume [21]

Ar	O ₂	H ₂ O	THC
Balance	2	3	0.5

3.1.1 Material selection

99.999% ultra-high purity argon (AR 5.0UH-T) was used as both the carrier and shielding gas for the DED experiments [21]. Its chemical composition is shown in Table 4.

Three hundred sixteen-liter stainless steel was chosen for the powder feedstock and substrate material for its popular use in manufacturing and relatively low cost. The metal powder used in this study is MetcoClad 316 L-Si manufactured by Oerlikon Metco [22]. Its chemical composition is shown in Table 5. Its particle size distribution is shown in Table 6. The substrates were cut from hot rolled, annealed bar stock to $74 \times 74 \times 6$ mm, and then ground to ensure that they were completely flat and level.

3.1.2 Experimental setup

The experimental setup inside of the machine is shown in Fig. 9. An in-house induction heating system was used for the experiments. All components were purchased off-the-shelf except for the induction coil and electronics housing, which were fabricated [23]. The heater system consists of a DC power supply, a zero-voltage switching (ZVS) inverter, a pancake induction coil made of hollow copper tubing, a water-cooling system for the coil, and a vortex tube spot cooler for the inverter electronics. An induction coil was placed directly beneath the substrate for preheating. The ZVS inverter and electronics were placed inside a metal housing to protect against laser reflections. Actuators were controlled by an Arduino Uno connected to solid state relays, which activate the DC power supply for the heater and compressed air to the vortex cooler. Two K-type thermocouples connected to a GraphTec GL850 DAQ were used to record temperature history of the substrate surface. The GraphTec was connected to a laptop running a Python controller script that communicates with the Arduino via a USB connection. The Python controller used a 6-s duty cycle where the heater was turned off for the first second to ensure an

Table 5 Chemical composition of MetcoClad 316 L-Si in weight percent [22]

Fe	Ni	Cr	Mo	Si	Mn	C	Others
Balance	12.0	17.0	2.5	2.3	1.0	0.03	≤0.5

Table 6 Particle size distribution of MetcoClad 316 L-Si [22]

Nominal range (μm)	Particle size distribution, weight %		
	+ 106 μm	− 106 + 44 μm	− 44 μm max
−106 + 44	5	90	5

accurate temperature reading. The controller allows for the input of a desired temperature, and the heater can be turned on for up to 5 out of every 6 s until this temperature is reached. The GraphTec, Arduino, and laptop setup outside of the machine is shown in Fig. 10.

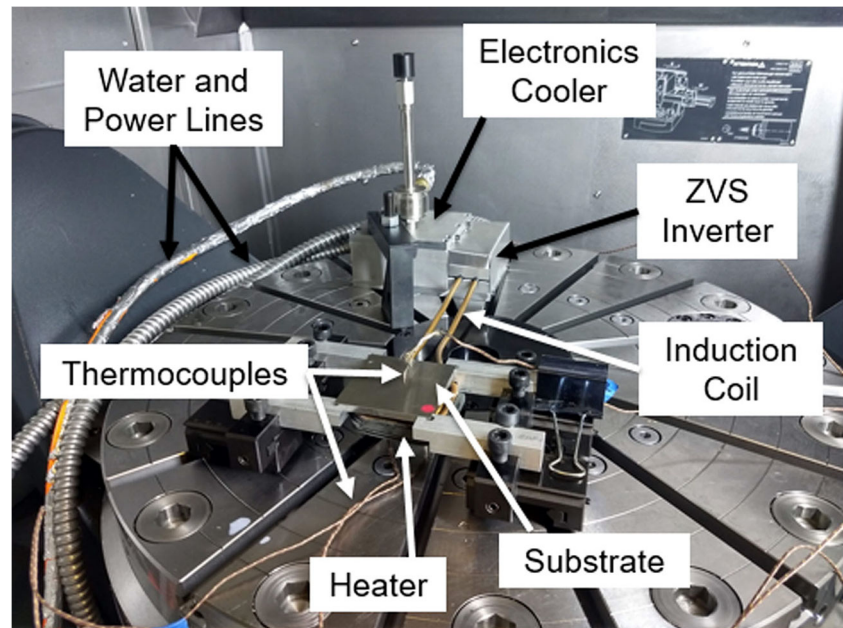
Six single line deposition experiments were performed on each substrate, spaced 10 mm apart, to conserve substrate material. Thermocouple placement is shown in Fig. 11. The controlled preheat temperature was always taken from the thermocouple located in the center of the substrate, with the second thermocouple reading used to ensure the preheat temperature was being measured accurately and that the temperature gradient across the substrate surface was never too large. The greatest difference observed between the two thermocouple readings during experiments was approximately 80 °C.

3.1.3 Clad geometry measurement

After depositions were completed, each clad was scanned using a Micro-Vu Excel 502HC metrology system to obtain their topology data. The x-, y-, and z-coordinates of the clad cross sections were measured perpendicular to the feed direction using laser scan lines that were duplicated at 0.1-mm intervals across the length of the clad. The scan pattern is shown in Fig. 12.

Once the clad measurements were taken, the coordinates were analyzed to find the height and width of each deposition using MATLAB. First, the code identifies and stores the x-, y-, and z-coordinates from each scan into separate vectors. The z-coordinates are then shifted so that the lowest point of the clad is at 0 because the top surface of the substrate does not always align with the x-y plane. A 3D surface plot of the original data is created with the x-y plane highlighted so that the original substrate surface can be seen more clearly. The substrates always show some amount of deflection, depending on the preheat temperature. To make sure the height and width measurements were accurate, the data on the sides was manually truncated to where the substrate remained relatively flat. The remaining middle section of the clad was used to find geometry measurements. Figure 13 shows examples of small and large deflections of the substrate that can be seen in the original Micro-Vu scans, as well as the cutoffs for where the data was truncated.

Fig. 9 Experimental setup inside of LASERTEC 65 3D



Next, the code loops through the data two times to remove duplicate data points. Then a fast Fourier transform is used to smooth and filter the data because the original data is very noisy. From this filtered data, the clad geometry can be calculated.

For each deposition, the data is divided into scan lines that are perpendicular to the feed direction. The way the height is measured is by finding the highest point in each of these scans, putting them into a matrix, and averaging all of the values. The width is measured by first identifying a threshold z value to ignore the noisy data at the edges of the clad. The intersection points of this threshold and the scan line are taken as the edges of the clad, and the difference between these two points is

stored in a matrix for each scan. The difference, or width, matrix is then averaged to find the width of the clad. Figure 14 illustrates the width calculation method.

4 Substrate preheat experiments

4.1 Overview and process parameters

The initial round of single line deposition experiments was performed with a preheated substrate and constant DED process parameters, which are shown in Table 7.

Fig. 10 Experimental setup outside of machine

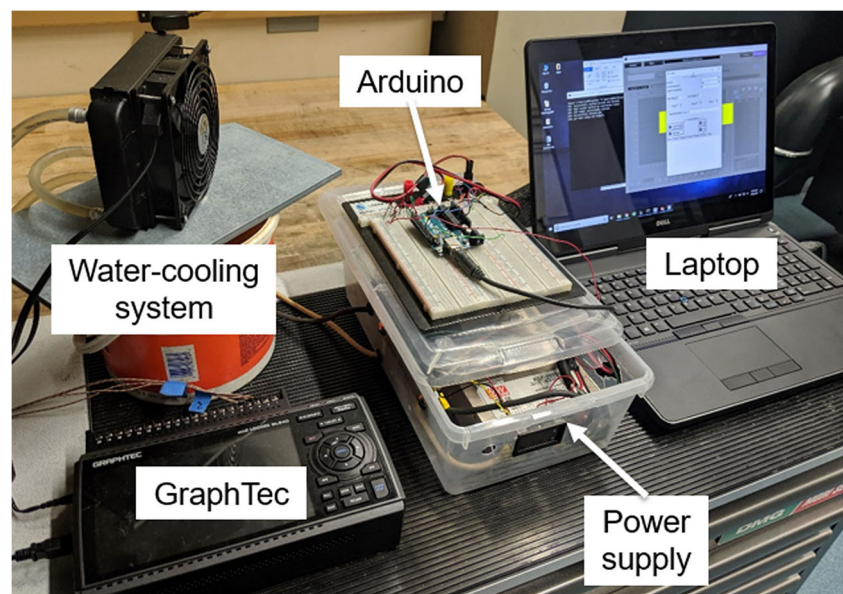
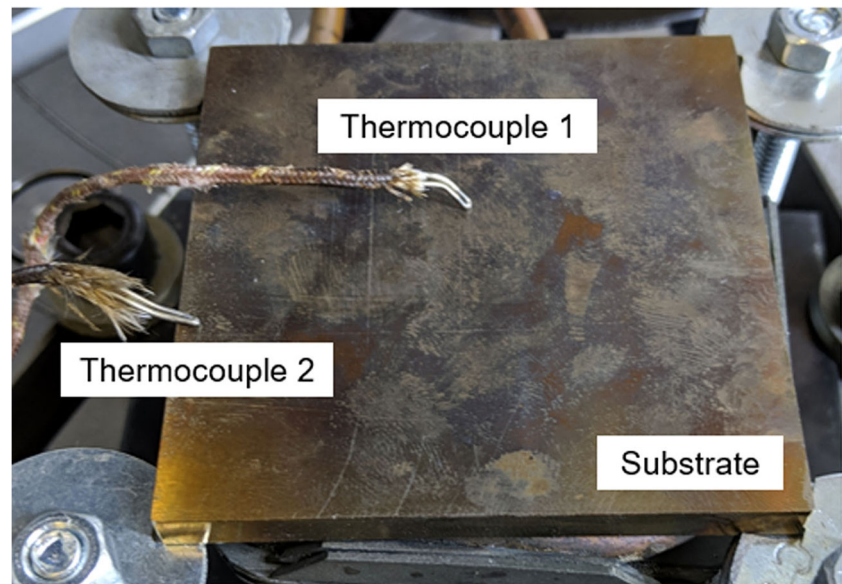


Fig. 11 Sample substrate showing thermocouple placement



The maximum temperature that the heater was able to achieve for these experiments was tested by setting the controller temperature to 500 °C and turning the heater on long enough for it to reach steady state. Once the heat loss due to convection becomes large enough, the heater is no longer able to increase the temperature of the substrate, which occurred at about 450 °C. The preheat temperatures tested were room temperature (23 °C) and 100–450 °C in approximately 50° increments. The actual deposition preheat temperature varied from the set temperature due to the time delay between when the substrate reached the desired temperature and when the deposition program was manually initialized. There was a 10-s dwell where argon gas and powder flow from the nozzle cooled the surface of the substrate immediately prior to deposition, which also affected the preheat temperature. All tested substrate temperatures are shown in Table 8.

4.2 Experimental results

All clad geometry results are shown in Table 9. Height and width values were found using MATLAB, and the cross-sectional area was estimated using the semi-ellipse area formula. To illustrate the area calculation, the cross

section of the clad is shown in Fig. 15. Equation 8 shows the area formula where h is clad height (mm) and w is clad width (mm).

The following figures show the relationships between the substrate temperatures and the geometry results.

The clad width results show an increasing trend as substrate temperature increases (Fig. 16). The relationship is logarithmic, and the fit line equation is shown in Eq. 9, where w is clad width (mm) and T is substrate temperature (°C). The R^2 value for this fit line is 0.7248.

$$A = \frac{\pi}{2} \cdot h \cdot \frac{w}{2} = \frac{\pi \cdot h \cdot w}{4} \quad (8)$$

$$w = 0.1808 \ln T + 2.1037 \quad (9)$$

With the increase in width and decrease in height as substrate temperature increases, it follows that the clad cross-sectional area should stay roughly constant across all experiments. The area does not vary by more than $\pm 7\%$ from the mean value of 1.49mm². A constant powder flow rate and powder flux were used for all substrate preheat experiments, which means that the same amount of powder was always delivered to the clad. Since the area of the clad remained



Fig. 12 Micro-Vu laser scanning pattern (not to scale)

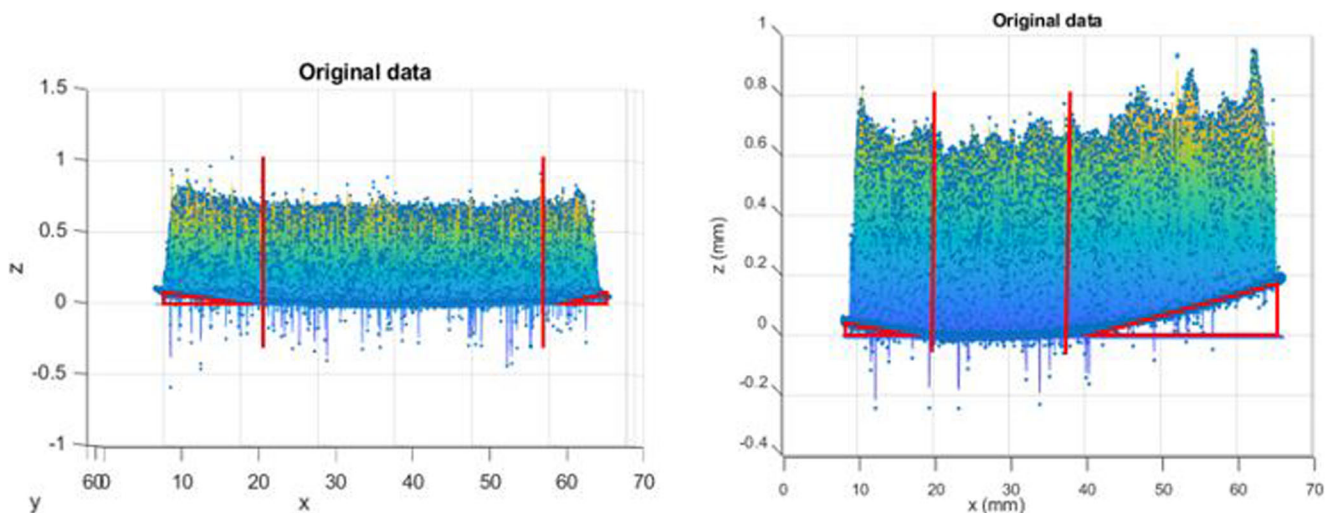


Fig. 13 Example 3D original laser scan data with small substrate deflection (left) and large substrate deflection (right). Red vertical lines indicate where data was truncated and only the middle section was analyzed

constant for all substrate temperatures, the same amount of metal powder was melted for each experiment, which implies that the efficiency of the depositions did not change. The cross-sectional area results show that the substrate temperature does not have a significant effect on the deposition efficiency (Fig. 17).

5 Laser power modulation experiments

5.1 Overview and process parameters

The second round of experiments that was performed used the same initial parameters as the previous round, except the laser power was decreased from 1200 W as substrate temperature was increased above room temperature. This method was used to test the theory that if total energy is

kept constant, clad geometry can be kept constant. As substrate energy increases, laser energy can be decreased, but since a method to experimentally calculate substrate energy has not yet been determined in this study, previous experimental lab data was used to estimate the initial change in laser power.

5.2 Experimental results

All clad geometry results are shown in Table 10. The cross-sectional area was again estimated using the semi-ellipse area formula shown in Eq. 8.

Since the purpose of these experiments was to reproduce the geometry obtained with the room temperature substrate preheat experiment, the experiments where this goal was achieved are highlighted in green in Table 10. Width of the clad is mainly influenced by changes in energy, so width was

Fig. 14 Clad width calculation method

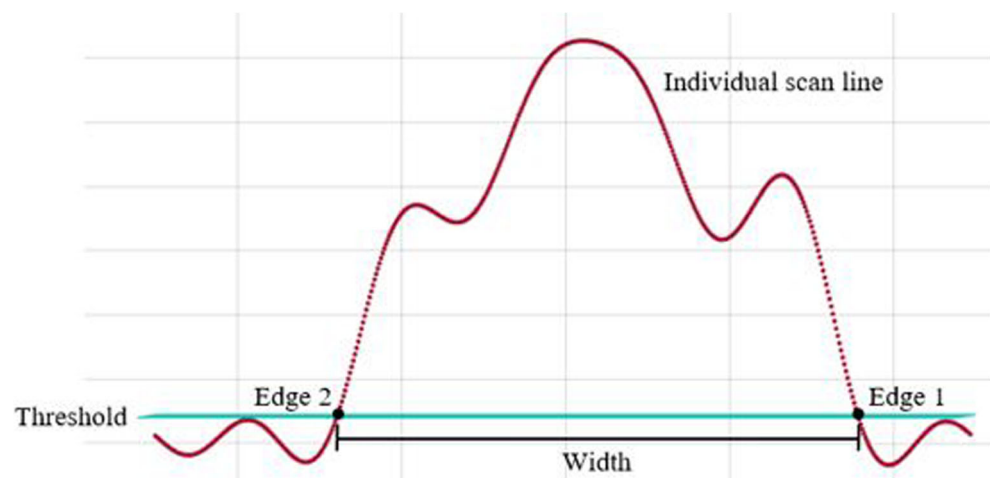


Table 7 Process parameters for substrate preheat experiments

Laser power (W)	Feed rate (mm/min)	Powder flow rate (g/min)	Clad length (mm)
1200	1000	13.5	54

the only geometric indicator considered when determining which experiments matched the desired geometry. The desired width from the room temperature substrate preheat experiment was 2.745 mm. Any clad from the laser power experiments that had a width within ± 70 μm of the desired value was considered to match to account for any variations or errors in experimentation or measurements.

Figures 18, 19, and 20 illustrate the relationships between the geometric indicators, energy flux, and substrate temperatures with 3D plots. The (x, y) coordinates are labeled next to the data points.

The clad height decreases as substrate temperature increases, which is consistent with the results found in Section 4.2.

The clad width stays more consistent, which was the goal of these experiments. There is a slight decreasing trend as substrate temperature increases and energy flux decreases.

The cross-sectional area of the clad consistently decreases as substrate temperature increases, and energy flux decreases mainly due to the change in height. These results show that a decrease in laser power, or energy flux, causes a decrease in deposition efficiency because it was determined in Section 4.2. that changes in substrate temperature do not significantly affect the deposition efficiency.

Table 8 Experimental substrate preheat temperatures

Target substrate temperature (°C)	Measured substrate temperature (°C)
23	23
100	92
100	109
150	137
150	150
200	197
200	209
200	215
250	237
250	250
250	261
300	277
300	306
350	320
400	361
450	435

6 Discussion

6.1 Controlling clad geometry

The results of the laser power modulation experiments showed the influence of changes in laser power, energy flux, and substrate temperature on clad geometry. Relationships between these DED parameters and the geometric indicators can be developed so that the overall geometry of a deposition can be predicted and controlled using desired inputs. Clad width and height are plotted in Figs. 21 and 22, respectively, against energy flux and substrate temperature with surface fits developed using MATLAB.

The surface fits are linear models using a polynomial with 3 degrees in x (substrate temperature) and 2 degrees in y (energy flux). The R^2 value for this fit is 0.8103, and the sum of squares due to error (SSE) is 0.3212. Equation 10 shows the surface fit equation for Fig. 21 where w is the clad width (mm), T_s is the substrate temperature (°C), and EF is the laser energy flux (kJ/cm²).

$$w = -1.303 + 0.007176T_s + 3.482EF - 4.556 \cdot 10^{-6}T_s^2 - 0.002501T_sEF - 0.7506EF^2 - 6.441 \cdot 10^{-9}T_s^3 + 2.81 \cdot 10^{-6}T_s^2EF + 3.51 \cdot 10^{-5}T_sEF^2 \tag{10}$$

Table 9 Clad geometry results

Substrate temperature (°C)	Clad height (mm)	Clad width (mm)	Cross-sectional area (mm ²)
23	0.6466	2.7450	1.3940
92	0.6704	2.9508	1.5537
109	0.6469	2.8836	1.4651
137	0.6384	2.7638	1.3858
150	0.6429	2.9817	1.5056
197	0.6271	3.1531	1.5530
209	0.6459	3.0656	1.5551
215	0.6183	3.1369	1.5233
237	0.5936	3.0650	1.4289
250	0.6193	3.0705	1.4935
261	0.6045	3.2128	1.5254
277	0.6267	3.0898	1.5208
306	0.6068	3.1343	1.4937
320	0.6017	3.1448	1.4862
361	0.5908	3.1935	1.4818
435	0.5708	3.2364	1.4509

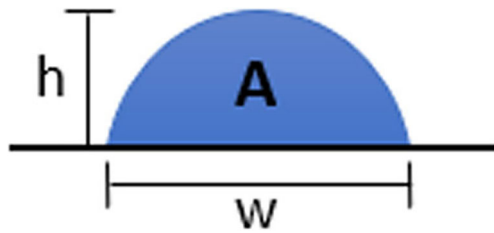


Fig. 15 Cross-sectional view of the clad showing how width and height were measured

Equation 11 shows the surface fit equation for clad height from Fig. 22. The R^2 value for the height fit is 0.7714, and the SSE is 0.0185.

$$h = -0.2648 + 0.00642T_s + 0.09842EF - 8.31 \cdot 10^{-6}T_s^2 - 0.005561T_sEF - 0.2521EF^2 + 2.983 \cdot 10^{-9}T_s^3 + 2.508 \cdot 10^{-6}T_s^2EF + 0.00125T_sEF^2 \quad (11)$$

Equations 10 and 11 can be used to estimate clad width and height for any substrate temperature up to about 400 °C and for energy flux values ranging from 1.0 to 2.4 kJ/cm². They can also be used to estimate the necessary preheat temperature or energy flux required to achieve a desired deposition width or height. This information is useful for multilayer depositions where adjustments need to be made to the energy flux between layers to keep clad width constant.

6.2 Relationship between substrate energy and clad geometry

The laser power modulation experiments where the desired geometry was achieved can be used to predict the relationship between substrate energy and clad geometry. Since the room temperature substrate clad width was reproduced with higher temperature substrates, it can be assumed that the total energy from Eq. 2 was kept constant at 2.4 kJ/cm² for these experiments. That means that the energy added to the substrate

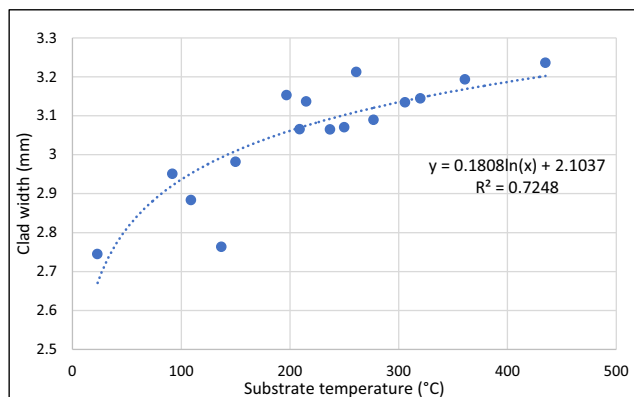


Fig. 16 Clad width results versus substrate temperature

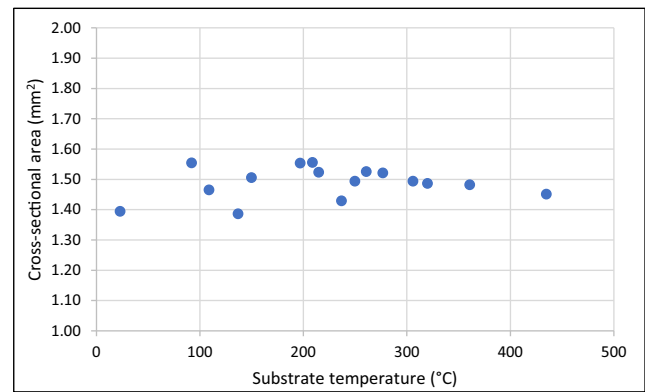


Fig. 17 Clad cross-sectional area results versus substrate temperature

should be equivalent to the reduction in laser energy, and using this idea, a method for quantifying the substrate energy can be determined. The substrate energy at room temperature is assumed to be zero. The successful laser power experimental results along with substrate energy flux calculations are shown in Table 11.

Using the estimates for substrate energy flux, an equation can now be developed to convert substrate temperature to energy per unit area. By plotting the substrate energy flux versus the substrate temperature from the laser power modulation experiments, a line can be fit to the data to find the relationship between the two. This plot is shown in Fig. 23.

The fit line equation, Eq. 12, can be used to calculate substrate energy per unit area given substrate temperature, where EF_s is the substrate energy flux (kJ/cm²) and T_s is the substrate temperature (°C). The R^2 value of the fit is 0.9338.

$$EF_s = 0.4841 \ln T_s - 1.5674 \quad (12)$$

This relationship can be used to convert the substrate temperatures used in the substrate preheat experiments to energy flux so that the relationship between substrate energy and clad geometry can be seen. Since Eq. 12 was developed using results from the laser power modulation experiments where the width of the clad matched the desired geometry, only the width can be compared with substrate energy calculations. Conclusions about the relationships between substrate energy and clad height or cross-sectional area cannot be made from these results. The clad width results from the substrate preheat experiments are plotted versus the converted substrate energy flux values in Fig. 24.

The fit line from Fig. 24 can be used to estimate the clad width given a substrate energy flux value. The fit line equation is shown in Eq. 13.

$$w = 0.1937EF_s^2 + 0.1104EF_s + 2.7403 \quad (13)$$

Table 10 Clad geometry results for laser power modulation experiments with experiments where goal geometry was achieved highlighted in green

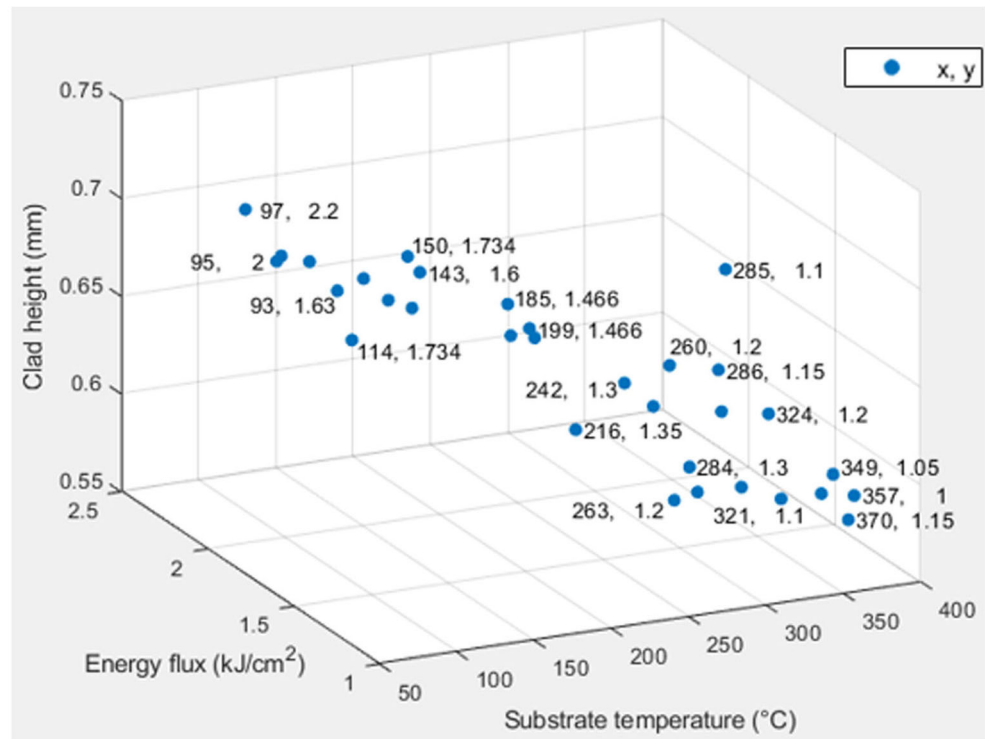
Substrate temperature (°C)	Laser power (W)	Energy flux (kJ/cm ²)	Clad height (mm)	Clad width (mm)	Area (mm ²)
93	815	1.630	0.6986	2.734	1.5001
94	900	1.800	0.7034	2.8223	1.5592
95	1000	2.000	0.6917	2.7852	1.5131
97	1100	2.200	0.7062	2.9318	1.6261
98	1000	2.000	0.694	2.9663	1.6168
110	815	1.630	0.7027	2.7558	1.5209
114	867	1.734	0.6648	2.9712	1.5514
130	833	1.666	0.6873	2.7376	1.4778
138	800	1.600	0.6862	2.7249	1.4686
143	800	1.600	0.7038	2.7012	1.4931
150	867	1.734	0.7031	2.8732	1.5866
174	675	1.350	0.6824	2.5851	1.3855
185	733	1.466	0.6904	2.5963	1.4078
195	700	1.400	0.6758	2.6518	1.4075
199	733	1.466	0.6763	2.8892	1.5346
216	675	1.350	0.6292	2.8711	1.4188
242	650	1.300	0.6529	2.9012	1.4877
255	625	1.250	0.6423	2.806	1.4155
260	600	1.200	0.6657	2.6439	1.3823
263	600	1.200	0.5964	2.7824	1.3033
278	600	1.200	0.5988	2.9171	1.3719
284	650	1.300	0.6049	2.8046	1.3324
285	550	1.100	0.7176	2.6672	1.5032
286	575	1.150	0.6632	2.6456	1.3780
288	575	1.150	0.6416	2.6454	1.3330
312	625	1.250	0.5943	2.8877	1.3479
321	550	1.100	0.596	2.5928	1.2137
324	600	1.200	0.6332	2.7205	1.3529
347	550	1.100	0.5956	2.8229	1.3205
349	525	1.050	0.6081	2.6908	1.2851
357	500	1.000	0.5993	2.4998	1.1766
370	575	1.150	0.5765	2.83	1.2814

The relationships between substrate energy and clad geometry developed in this section give an idea as to how the energy per unit area of the substrate or previously deposited layer of a part influences the clad width. This information can be used to predict changes in clad width during DED or to produce a desired width from given input parameters.

6.3 Deposition efficiency

Altering DED process parameters can change the deposition efficiency. Factors such as conduction, convection, absorption, and attenuation contribute to efficiency of energy delivery to the clad. During the substrate preheat experiments, it

Fig. 18 Clad height versus energy flux and substrate temperature



was noted that changes in substrate temperature do not significantly affect efficiency due to the cross-sectional area remaining constant even though the height and width changed. This means that the total amount of powder that was melted stayed roughly constant for all substrate temperatures. A higher

substrate temperature also means that the cooling rate is decreased, which is beneficial for deformation and material properties of the work piece.

The laser power modulation experiments involved adjusting only the laser power and substrate temperature,

Fig. 19 Clad width versus energy flux and substrate temperature

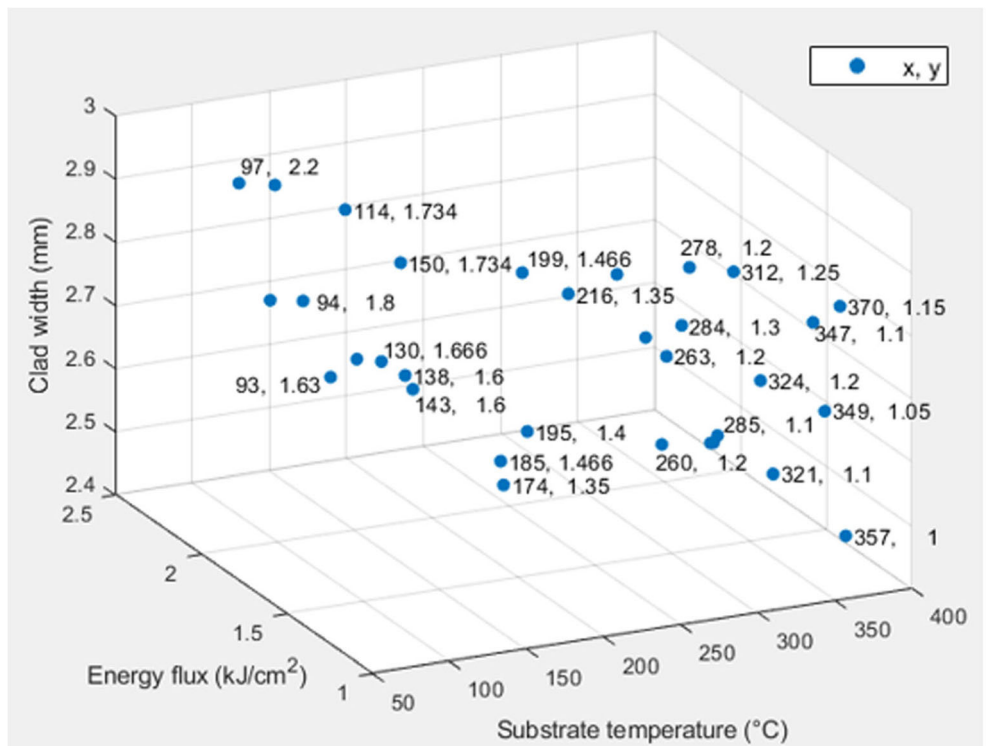
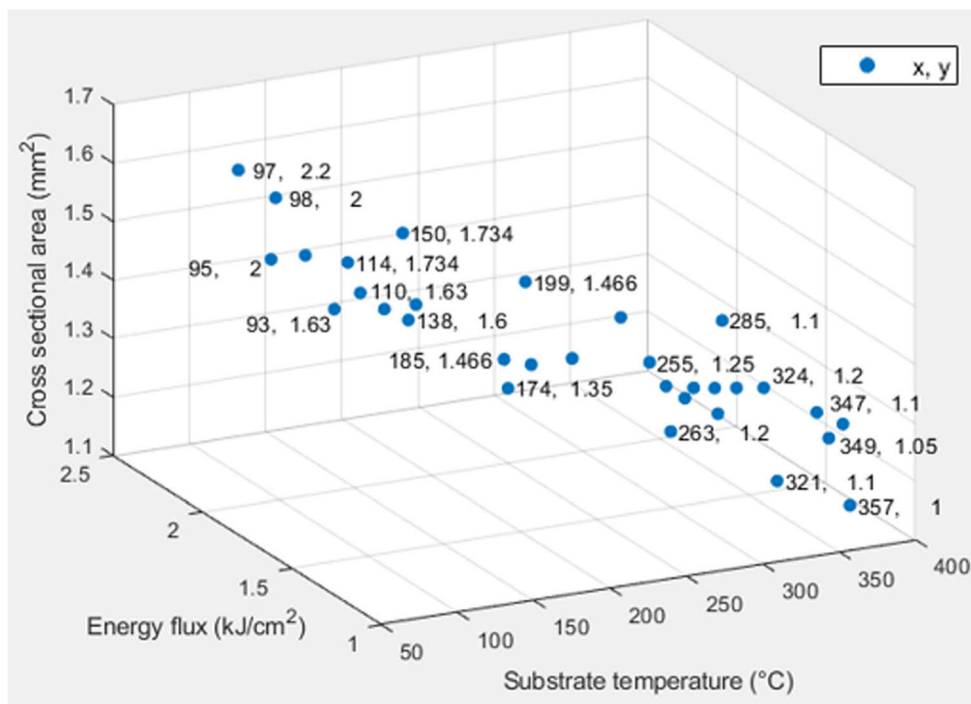


Fig. 20 Clad cross-sectional area versus energy flux and substrate temperature



while all other parameters stayed the same. The cross-sectional area of the clad did not remain constant, so the changes in laser power were the cause for this change in efficiency. A decrease in laser power and therefore energy flux resulted in a smaller cross-sectional clad area. The reason for this may be that when a lower laser power is

used, there is less energy available to be absorbed by the same amount of powder and less powder is melted into the clad. There is also less energy available to be absorbed into the substrate, which means the powder may not be able to bond as well with the substrate material even with preheating.

Fig. 21 Clad width data from laser power modulation experiments versus laser energy flux and substrate temperature with surface fit

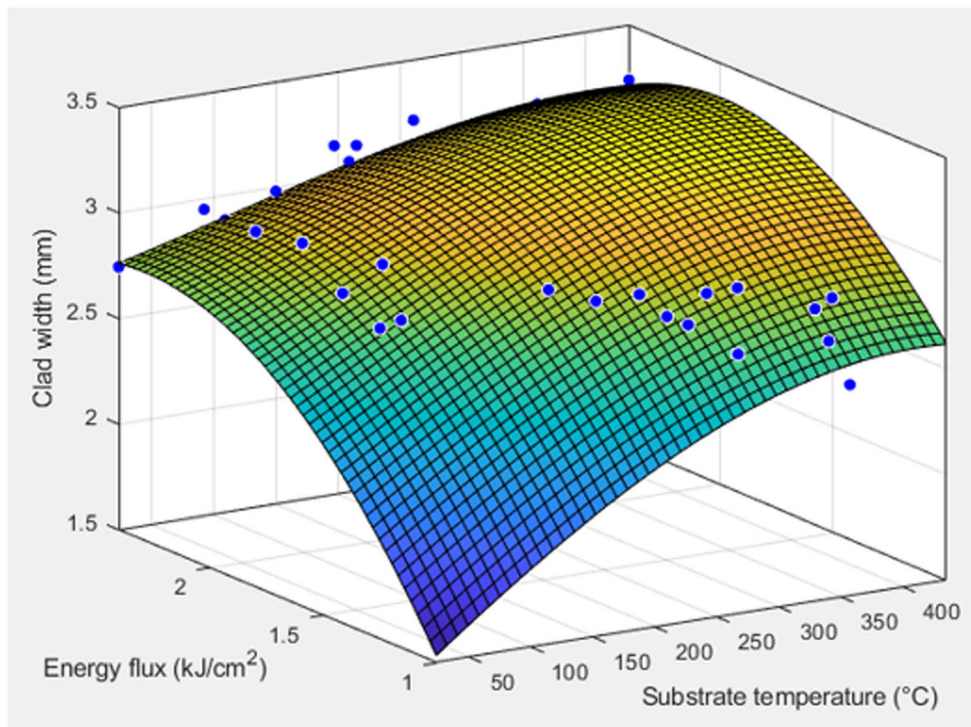
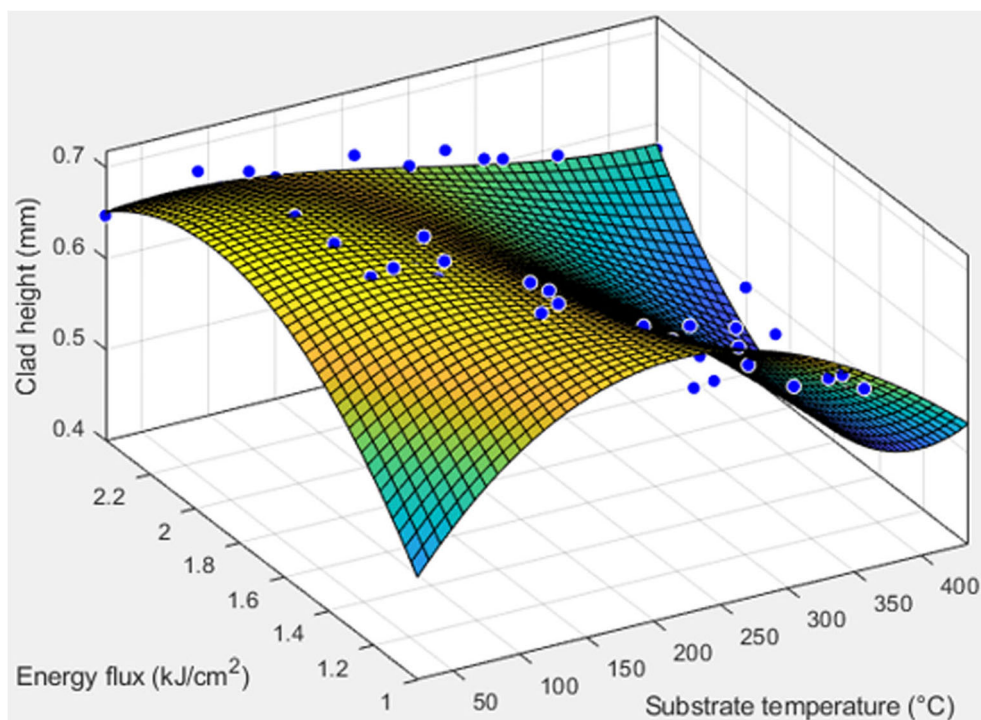


Fig. 22 Clad height data from laser power modulation experiments versus laser energy flux and substrate temperature with surface fit



7 Summary and future work

7.1 Summary

This study presented a preliminary method to control clad geometry. The influence of altering the process parameters and preheating the substrate during DED on clad geometry was measured. It was found that an increase in substrate temperature results in an increase in clad width and a decrease in clad height. Discoveries were made about how the deposition efficiency, which should be taken into consideration when deciding on process parameter values, is affected by changes in substrate temperature and laser power. Changes in substrate

temperature do not influence the deposition efficiency, while a decrease in laser power causes a decrease in the efficiency. Equations were developed to predict the clad height and width when using different substrate preheat temperatures and energy flux values. A relationship between the substrate energy and clad width was also found so that changes in clad width during the deposition process can be predicted. These results are a step toward more accurate DED part geometry because they can be used during multilayer depositions to keep the geometry of each track consistent.

7.2 Future work

The influence of substrate energy on clad height is still unclear. In the future, more experimentation is necessary to find the relationship between substrate energy and clad height so

Table 11 Successful laser power modulation experimental results

Substrate temperature (°C)	Laser power (W)	Energy flux (kJ/cm ²)	Clad height (mm)	Clad width (mm)	Cross-sectional area (mm ²)	Substrate energy flux (kJ/cm ²)
93	815	1.630	0.6986	2.7340	1.5001	0.77
95	1000	2.000	0.6917	2.7852	1.5131	0.400
110	815	1.630	0.7027	2.7558	1.5209	0.770
130	833	1.666	0.6873	2.7376	1.4778	0.734
138	800	1.600	0.6862	2.7249	1.4686	0.800
143	800	1.600	0.7038	2.7012	1.4931	0.800
255	625	1.250	0.6423	2.8060	1.4155	1.150
263	600	1.200	0.5964	2.7824	1.3033	1.200
284	650	1.300	0.6049	2.8046	1.3324	1.100
324	600	1.200	0.6332	2.7205	1.3529	1.200
349	525	1.050	0.6081	2.6908	1.2851	1.350

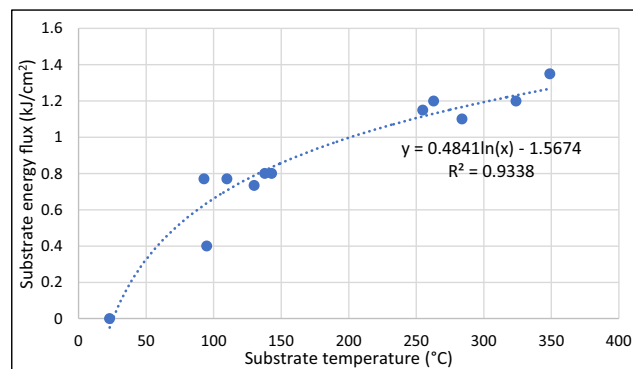


Fig. 23 Substrate energy flux versus substrate temperature

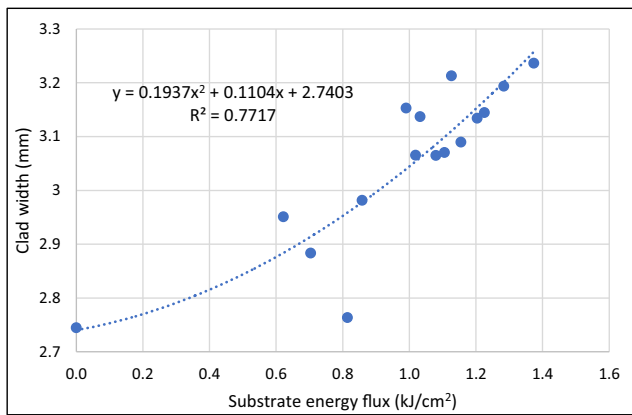


Fig. 24 Substrate preheat experimental clad width results versus substrate energy flux

that the influence of substrate energy on total clad geometry can be understood. The methods for controlling clad geometry could also be expanded upon by performing tests with higher substrate temperatures, as the induction heater used in this study was only able to heat the substrate to a maximum temperature of 435 °C. Clad geometry data for higher substrate temperatures could be useful for controlling the geometry of multilayer parts because the temperature of each layer can be much hotter than 435 °C during deposition.

Changes in process parameters can affect material properties such as density, porosity, and grain morphology. The quality of each deposition was not assessed and should be analyzed in future testing. Thermal gradient, cooling rate, and solidification rate all contribute to deflection of the work piece but were not considered in this study. Substrate deflection with different substrate preheat temperatures and process parameters should also be analyzed.

Acknowledgments The authors would like to thank DMG Mori and MTTRF for their support of the ARMS lab.

References

- Prakash KS, Nancharaih T, Rao VS (2018) Additive manufacturing techniques in manufacturing - an overview. *Mater Today Proc* 5(2): 3873–3882
- Thompson SM, Bian L, Shamsaeii N, Yadollahi A (2015) An overview of direct laser deposition for additive manufacturing; part I: transport phenomena, modeling and diagnostics. *Addit Manuf* 8: 36–62
- Foteinopoulos P, Papacharalampopoulos A, Stavropoulos P (2018) On thermal modeling of additive manufacturing processes. *CIRP J Manuf Sci Technol* 20:66–83
- Majeed M, Khan H, Rasheed I (2019) Finite element analysis of melt pool thermal characteristics with passing laser in SLM process. *Optik* 194
- Huang W, Zhang Y (2019) Finite element simulation of thermal behavior in single-track multiple-layers thin wall without-support during selective laser melting. *J Manuf Process* 42:139–148
- Huang Y, Yang L, Du X, Yang Y (2016) Finite element analysis of thermal behavior of metal powder during selective laser melting. *Int J Therm Sci* 104:146–157
- Manvatkar V, De A, DebRoy T (2015) Spatial variation of melt pool geometry, peak temperature and solidification parameters during laser assisted additive manufacturing process. *Mater Sci Technol* 31(8):924–930
- Yan Z, Liu W, Tang Z, Liu X (2018) Review on thermal analysis in laser-based additive manufacturing. *Opt Laser Technol* 106:427–441
- Tang L, Landers RG (2010) Melt pool temperature control for laser metal deposition processes—part II: layer-to-layer temperature control. *J Manuf Sci Eng* 132(1)
- Muller AV, Schlick G, Neu R, Anstatt C (2019) Additive manufacturing of pure tungsten by means of selective laser beam melting with substrate preheating temperatures up to 1000°C. *Nucl Mater Energy* 19:184–188
- Zhang K, Wang S, Liu W, Long R (2014) Effects of substrate preheating on the thin-wall part built by laser metal deposition shaping. *Appl Surf Sci* 317:839–855
- Fallah V, Alimardani M, Corbin SF, Khajepour A (2010) Impact of localized surface preheating on the microstructure and crack formation in laser direct deposition of Stellite 1 on AISI 4340 steel. *Appl Surf Sci* 257(5):1716–1723
- (1979) High-temperature characteristics of stainless steels. In: A Designer's handbook series. American Iron and Steel Institute, Washington DC
- Mills KC (2002) Recommended values of Thermophysical properties for selected commercial alloys. Woodhead Publishing Limited, Sawston
- Carter D (2017) A study on CAM based path planning for hybrid machining center with direct energy deposition. Master's thesis, Davis, CA
- Miettinen J, Louhenkilpi S (1994) Calculation of thermophysical properties of carbon and low alloyed steels for modeling of solidification processes. *Metall Mater Trans B* 25B:909–916
- Lindgren LE (2007) Computational welding mechanics: thermomechanical and microstructural simulations. Woodhead Publishing, New York
- Lia F, Park J, Tressler J, Martukanitz R (December 2017) Partitioning of laser energy during directed energy deposition. *Addit Manuf* 18:31–39
- Heigel JC (2018) Chapter 8 - thermo-mechanical modeling of thin wall builds using powder fed directed energy deposition. In: Thermo-mechanical modeling of additive manufacturing. The Pennsylvania State University, University Park, pp 137–151
- LASERTEC 65 3D Hybrid. DMG Mori, [Online]. Available: <https://us.dmgmori.com/products/machines/additive-manufacturing/powder-nozzle/lasertec-65-3d-hybrid>. Accessed 2019
- Argon. Praxair, [Online]. Available: <https://www.praxair.com/-/media/corporate/praxairus/documents/specification-sheets-and-brochures/gases/argon/argon-ar-spec-sheet-ss-p4563.pdf?la=en&rev=d86586a5926d487ea3f79476f0d84838>. Accessed 2019
- Material Product Data Sheet: Austenitic Stainless Steel Powder for Laser Cladding. Oerlikon Metco, [Online]. Available: https://www.oerlikon.com/ecomaXL/files/metco/oerlikon_DSMW-0017.2_AusteniticSteel_LC.pdf. Accessed 2019
- Odum KS (2019) Method to reduce final part deformation using thermal control of the directed energy deposition process. PhD dissertation, Davis, CA

Publisher's note Springer Nature remains neutral with regard to jurisdictional claims in published maps and institutional affiliations.